A novel role of the interferon-inducible protein IFI16 as inducer of proinflammatory molecules in endothelial cells

(Article begins on next page)

20 July 2024

A Novel Role of the Interferon-inducible Protein IFI16 as Inducer of Proinflammatory Molecules in Endothelial Cells*

Patrizia Caposio[‡], Francesca Gugliesi[‡], Claudia Zannetti[‡], Simone Sponza[‡], Michele Mondini[‡§], Enzo Medico[¶], John Hiscott[‖], Howard A. Young[**], Giorgio Gribaudo[‡], Marisa Gariglio[§], and Santo Landolfo[‡1]

From the [‡]Department of Public Health and Microbiology and the [¶]Institute for Cancer Research and Treatment, University of Turin, Turin 10126, Italy, the [‖]Lady Davis Institute, McGill University, Montreal H3T 1E2, Canada, the [**]Laboratory of Experimental Immunology, Center for Cancer Research, NCI-Frederick, National Institutes of Health, Frederick, Maryland 21702, and the [§]Department of Clinical and Experimental Medicine, University of Piemonte Orientale, 28100 Novara, Italy

The human *IFI16* gene is an interferon-inducible gene implicated in the regulation of endothelial cell proliferation and tube morphogenesis. Immunohistochemical analysis has demonstrated that this gene is highly expressed in endothelial cells in addition to hematopoietic tissues. In this study, gene array analysis of human umbilical vein endothelial cells overexpressing IFI16 revealed an increased expression of genes involved in immunomodulation, cell growth, and apoptosis. Consistent with these observations, IFI16 triggered expression of adhesion molecules such as ICAM-1 and E-selectin or chemokines such as interleukin-8 or MCP-1. Treatment of cells with short hairpin RNA targeting IFI16 significantly inhibited ICAM-1 induction by interferon (IFN)-γ demonstrating that IFI16 is required for proinflammatory gene stimulation. Moreover, functional analysis of the ICAM-1 promoter by deletion- or site-specific mutation demonstrated that NF-κB is the main mediator of IFI16-driven gene induction. NF-κB activation appears to be triggered by IFI16 through a novel mechanism involving suppression of IκBα mRNA and protein expression. Support for this finding comes from the observation that IFI16 targeting with specific short hairpin RNA down-regulates NF-κB binding activity to its cognate DNA and inhibits ICAM-1 expression induced by IFN-γ. Using transient transfection and luciferase assay, electrophoretic mobility shift assay, and chromatin immunoprecipitation, we demonstrate indeed that activation of the NF-κB response is mediated by IFI16-induced block of Sp1-like factor recruitment to the promoter of the *IκBα* gene, encoding the main NF-κB inhibitor. Activation of NF-κB accompanied by induction of proinflammatory molecules was also observed when IκBα expression was down-regulated by specific small interfering RNA, resulting in an outcome similar to that observed with IFI16 overexpression. Taken together, these data implicate IFI16 as a novel regulator of endothelial proinflammatory activity and provide new insights into the physiological functions of the IFN-inducible gene *IFI16*.

Interferons (IFNs)[2] are important regulators of viral replication, cell growth, immunomodulation, and inflammation (1, 2). Moreover, it is now well accepted that IFNs play a critical role in the pathogenesis and perpetuation of specific autoimmune diseases, including systemic lupus erythematosus, autoimmune thyroid disease, and type 1 diabetes (3).

The interferon-inducible p200 family of proteins (Ifi200 in the mouse and HIN200 in the humans) is among the numerous gene products induced by IFNs (4–6). Recently, the Pyrin domain, commonly found among cell death-associated proteins such as Pyrin, ASC, and zebrafish caspase, and also referred to as the PAAD/DAPIN domain (7, 8), has been found in the N terminus of most Ifi200/HIN200 proteins, suggesting a role of these proteins in inflammation and apoptosis (9, 10). The *IFI16* gene, a member of the HIN200 family (4–6), was originally identified as a target of interferons (IFN-α/β and -γ). Recently, however, it has become clear that oxidative stress, cell density, and various proinflammatory cytokines also trigger IFI16 expression (11, 12). IFI16 expression is seen in vascular endothelial cells from blood and lymph vessels in addition to hematopoietic cells, suggesting a possible link to angiogenesis and inflammation (13, 14). Consistent with this hypothesis, expression of IFI16 in HUVEC efficiently suppressed endothelial migration, invasion, and formation of capillary-like structures *in vitro* accompanied by inhibition of cycle progression and arrest in the G$_1$ phase of the cell cycle (15). Additionally, anti-IFI16 autoantibody titers are significantly elevated in patients with autoimmune diseases such as cutaneous systemic sclerosis, systemic lupus erythematosus, and Sjogren syndrome, but not in those with other autoimmune diseases when compared with controls (16). Taken together, these results indicate that IFI16 may be involved in the early steps of inflammation by modulating endothelial cell functions.

One of the initial key events in the endothelial response to inflammatory stimuli is the expression of adhesion molecules such as intercellular cell adhesion molecule (ICAM-1, VCAM-1,

[2] The abbreviations used are: IFN, interferon; HUVEC, human umbilical vein endothelial cell; siRNA, small interfering RNA; shRNA, short hairpin RNA; mAb, monoclonal antibody; FITC, fluorescein isothiocyanate; TNF, tumor necrosis factor; m.o.i., multiplicity of infection; RT, reverse transcription; ChIP, chromatin immunoprecipitation; IL, interleukin; PFU, plaque-forming unit; PBS, phosphate-buffered saline; EGM, endothelial growth medium; EMSA, electrophoretic mobility shift assay; IKK, IκB kinase; Ab, antibody; p.i., post-infection; h.p.i., hours p.i.; FACS, fluorescence-activated cell sorter.

and E-selectin) and production of chemokines, including IL-8 and MCP-1 (17–19). The majority of genes expressed in endothelial cells in response to inflammatory mediators such as lipopolysaccharide, IL-1β, or TNF-α contain functionally important NF-κB-binding sites in their promoter regions (20, 21). Moreover, inhibition of NF-κB activity resulted in efficient inhibition of endothelial cell activation (22–24). The five members of the mammalian NF-κB family, p65 (RelA), RelB, c-Rel, p50/p105 (NF-κB1), and p52/p100 (NF-κB2), are present in unstimulated cells as homo- or heterodimers bound to IκB family proteins (22–24). NF-κB proteins are characterized by the presence of a conserved 300-amino acid Rel homology domain that is located toward the N terminus of the protein and is responsible for dimerization, interaction with IκBs, and binding to DNA. Binding to IκB prevents the NF-κB-IκB complex from translocating to the nucleus, thereby maintaining NF-κB in an inactive state.

Three distinct NF-κB-activating pathways have emerged, and all of them rely on sequentially activated kinases (25–27). The first pathway, *i.e.* the classical pathway, is triggered by proinflammatory cytokines such as TNF-α and leads to the sequential recruitment of various adaptors, including TNF receptor-associated death domain protein, receptor interacting protein, and TNF receptor-associated factor 2 (TRAF2) to the cytoplasmic membrane. This is followed by the recruitment and activation of the IκB kinase (IKK) complex, which includes the scaffold protein NF-κB essential modulator (NEMO; also named IKKγ), IKKα, and IKKβ kinases. Once activated, the IKK complex phosphorylates on Ser-32 and Ser-36 IκBα, which is subsequently ubiquitinated and then degraded via the proteosome pathway. A second pathway, *i.e.* the alternative pathway, is NEMO-independent and is triggered by cytokines, including lymphotoxin b, B-cell activating factor or the CD40 ligand, and by viruses (*e.g.* human T-cell leukemia virus and the Epstein-Barr virus). This pathway relies on the recruitment of TRAF proteins to the membrane and on the NF-κB-inducing kinase (NIK), which activates an IKKα homodimer. IKKα phosphorylates the ankyrin-containing and inhibitory molecule p100 on specific serine residues located in both the N- and C-terminal regions. p100 is then ubiquitinated and cleaved to generate the NF-κB protein p52 that moves as a heterodimer with RelB into the nucleus. The third signaling pathway is classified as "atypical" because it is independent of IKK but still requires the proteosome and is triggered by DNA-damaging agents such as UV radiation or doxorubicin. UV radiation induces IκBα degradation via the proteosome, but the targeted serine residues are located within a C-terminal cluster that is recognized by the p38-activated casein kinase 2 (CK2).

To add new information to the physiological role of IFI16 in the modulation of the immune response and inflammation, we initiated microarray analysis of IFI16-overexpressing HUVEC. The results obtained indicate that genes involved in inflammation, cell proliferation, and apoptosis are affected by IFI16 overexpression. In particular we demonstrate that IFI16 stimulates the expression of proinflammatory genes, including *ICAM-1*, E-selectin, *IL-8*, and *MCP-1*. ICAM-1 stimulation by IFNs appears to depend on functional IFI16, because inhibition of its expression by RNA interference blocks the IFN capability to increase ICAM-1 expression. ICAM-1 induction takes place through activation of the NF-κB complex that appears to be triggered by transcriptional suppression of the *IκBα* gene expression. Consistent with these observations, reduction in IκBα expression by RNA interference results in the same outcome observed with IFI16 overexpression. Altogether, these results demonstrate that IFI16 modulates the response of proinflammatory cytokines in endothelial cells and may provide a molecular explanation for its role in the initial steps of the autoimmune response.

EXPERIMENTAL PROCEDURES

Cells Lines and Reagents—HUVEC obtained by trypsin treatment of umbilical cord veins were cultured in endothelial growth medium (EGM-2, Clonetics, San Diego) containing 2% fetal bovine serum, human recombinant vascular endothelial growth factor, basic fibroblast growth factor, human epidermal growth factor, insulin growth factor (IGF-1), hydrocortisone, ascorbic acid, heparin, gentamycin, and amphotericin B (1 μg/ml each) and were seeded into 100-mm culture dishes coated with 0.2% gelatin. Experiments were performed with cells at passage 2–6. Human embryo kidney 293 cells (HEK-293) (Microbix Biosystems Inc.) were cultured in minimum Eagle's medium (Invitrogen) supplemented with 10% fetal bovine serum (Invitrogen), 2 mM glutamine, 100 units of penicillin per ml, and 100 μg per ml of streptomycin sulfate. Cells were kept in logarithmic growth phase by 1$\times$ citric saline detachment and reinoculation every 2–4 days. Interferon-γ and TNF-α were the generous gifts of Gianni Garotta, Geneva, Switzerland, and Tiziana Musso, Turin, Italy, respectively.

Recombinant Adenovirus Preparations and HUVEC Infection—The pAC-CMV IFI16, containing the human IFI16 cDNA linked to a FLAG tag at the N terminus, was cotransfected together with pJM17 into human embryonic kidney 293 cells as described previously (11). After several rounds of plaque purification, the adenovirus containing the *IFI16* gene (AdVIFI16) was amplified on 293 cell monolayers and purified from cell lysates by banding twice on CsCl gradients. Desalting was performed using G-50 columns (Amersham Biosciences), and viruses were frozen in PBS, 10% glycerol at $-80\,°C$. The infectious titers (PFU) were determined by a standard plaque assay on 293 cell monolayers (11). The physical particles of the vector preparations were measured by spectrophotometry (28), and our viral preparations showed a 1:10–1:20 ratio between PFU and physical particles. Endotoxin contaminations were excluded by E-Toxate kit (Sigma) (sensitivity > 1.4 pg/ml). Recombinant AdVIFI16 was tested for IFI16 expression by Western blotting, using an anti-FLAG antibody (Sigma). For cell transduction, pre-confluent HUVEC were washed once with PBS and incubated with AdVIFI16 or AdVLacZ (used as a control) at a multiplicity of infection (m.o.i.) of 300 in EGM. After 60 min at 37 °C, the virus was washed off, and fresh medium was added. Cells were cultured for 36 h before use in the experiments.

For IFI16 interference the pAC-CMV shRNA-IFI16, containing the short hairpin RNA sequence targeting the human *IFI16* gene mRNA (shRNAIFI16) (5′-CCG TCA GAA GAC CAC AAT CTA CTT CAA GAG AGT AGA TTG TGG TCT

TCT GAT TTT TTG GAA A-3′), or the pAC-CMV shRNA-SCRAMBLED (shRNASCR), containing a scrambled human *IFI16* gene shRNA sequence (5′-CCG GCA CAG TCA CAA CAA ATC TTT CAA GAG AAG ATT TGT TGT GAC TGT GCT TTT TTG GA AA-3′), were cotransfected with pJM17 into 293 cells. After several rounds of plaque purification, recombinant adenoviruses were amplified on 293 cell monolayers and purified to homogeneity as before. PFU were assessed for virus titers on the 293 complementing cell line with agar overlay. Recombinant AdVshRNAIFI16 was tested for IFI16 knockdown by Western blotting. For cell transduction, HUVEC were washed once with PBS and incubated with AdVshRNAIFI16 or AdVshRNASCR at an m.o.i. of 300 in EGM. After 2 h at 37 °C, the virus was washed off, and cells were treated as indicated. For IκBα interference, the adenoviral human IκBα siRNA recombinant virus (AdVshRNAIκBα) containing the short hairpin RNA sequence targeting the human IκBα gene mRNA was purchased from Imgenex (San Diego, CA) and used according to the manufacturer's instruction at an m.o.i. of 1000.

Microarray and Data Analysis—Total RNA was extracted from HUVEC cultured at subconfluence and infected with AdVIFI16 or AdVLacZ for 6 h or 24 h. RNA pooled from different cultures was used as a template for biotinylated probe synthesis. Total RNAs were quality-controlled and quantified on the Bioanalyzer 2100 (Agilent). For gene expression profiling on Beadchips from Illumina, reverse transcription, double-stranded cDNA, and biotinylated cRNA synthesis were carried out according to standard Illumina protocols, using the "Illumina RNA amplification kit" (Ambion) and biotin-16 UTP (Roche Applied Science). Briefly, 500 ng of total RNA were used for reverse transcription to synthesize double-stranded cDNA. The cDNA was used for *in vitro* transcription to obtain biotinylated cRNA, followed by a purification step. Subsequently, 550 ng of biotinylated cRNA, resuspended in Hyb E1 buffer, formamide, and RNase-free water, were denatured at 65 °C for 5 min and hybridized for 16 h at 55 °C on Ilumina "Human Sampler" bead arrays, exploring 516 genes. Hybridized bead arrays were then washed three times with E1BC buffer (Illumina), once with 100% EtOH, blocked using blocking E1 buffer (Illumina), and stained with streptavidin-Cy3 (2 μl per chip of 1 mg/ml stock, from Amersham Biosciences). After the final washing and drying, bead arrays were scanned on a GenePix Personal 4100A microarray reader (Axon). Images were processed with the Beadarray Studio software (Illumina) to extract signal intensities for each bead type in each experiment and export them to a tab-delimited text file. Statistical analysis and selection of regulated genes was carried out using Excel (Microsoft). We defined two criteria for selecting regulated genes as follows: (*a*) genes that were regulated more than 2-fold in both replicates (32 genes); (*b*) genes that were regulated by average at least 1.4-fold plus 2 standard deviations (45 genes). The first approach allowed capturing genes with greater response, and the second allowed identifying genes with smaller, but consistent, response. In total, we selected 55 genes, of which 22 passed both tests.

Real Time RT-PCR Analysis—RT-PCR analysis was performed on an Mx 3000 P^{TM} (Stratagene) using the SYBR Green I dye (Invitrogen) as a nonspecific PCR product fluorescence label. Total cellular RNA was isolated using the Eurozol reagent (Euroclone Ltd.). RNA (1 μg) was then retrotranscribed at 42 °C for 60 min in PCR buffer (1.5 mM MgCl$_2$) containing 5 μM random primers, 0.5 mM dNTP, and 100 units of Moloney murine leukemia virus reverse transcriptase (Ambion) in a final volume of 20 μl. cDNAs (2 μl) or water as control was amplified in duplicate by real time RT-PCR using the Brilliant SYBR Green QPCR master mix (Stratagene) in a final volume of 25 μl. Primer sequences were as follows: IFI16 (sense, 5′-ACT GAG TAC AAC AAA GCC ATT TGA-3′; antisense, 5′-TTG TGA CAT TGT CCT GTC CCC AC-3′); ICAM-1 (sense, 5′-CAA CCG GAA GGT GTA TGA AC-3′; antisense, 5′-CAG CGT AGG GTA AGG TTC-3′); V-CAM1 (sense, 5′-CAT GGA ATT CGA ACC ACA-3′; antisense, 5′-GAC CAA GAC GGT TGT ATC GG-3′); BAD (sense, 5′-CAT TGA GCC GAG TGA GCA GG-3′; antisense, 5′-TCG TCA CTC ATC CTC CGG AG-3′); UCP3 (sense, 5′-CGT GGT GAT GTT CGT AAC CTA TG-3′; antisense, 5′-CGG TGA TTC CCG TAA CAT CTG-3′); CDC25a (sense, 5′-CTC CTC CGA GTC AAC AGA TT-3′; antisense, 5′-CAG AGT TCT GCC TCT GTG TG-3′); SSTR1 (sense, 5′-GGC GAA ATG CGT CCC AG-3′; antisense, 5′-CGG AGT AGA TGA AAG AGA TCA GGA-3′); CCR4 (sense, 5′-CCT CAG AGC CGC TTT CAG A-3′; antisense, 5′-GCC TTG ATG CCT CTC TTG GT-3′); E-Selectin (sense, 5′-CTC TGA CAG AAG AAG CCA AG-3′; antisense, 5′-ACT TGA GTC CAC TGA AGT CA-3′); MCP-1 (sense, 5′-TCC TGT GCC TGC TGC TGA TAG C-3′; antisense, 5′-TTC TGA ACC CAC TTC TGC TTG G-3′); IL-8 (sense, 5′-ATG ACT TCC AAG CTG GCC GTG GCT-3′; antisense, 5′-TCT CAG CCC TCT TCA AAA ACT TCT C-3′); PAI-1 (sense, 5′-TGC TGG TGA ATG CCC TCT ACT-3′; antisense, 5′-CGG TCA TTC CCA GGT TCT CTA-3′); PTX-3 (sense, 5′-TGG CTG CCG GCA GGT; antisense, 5′-TCC ACC CAC CAC AAA CAC TAT-3′); and β-actin (sense, 5′-GTT GCT ATC CAG GCT GTG-3′; antisense, 5′-TGT CCA CGT CAC ACT TCA-3′). Following an initial denaturing step at 95 °C for 2 min to activate 0.75 units of Platinum *Taq* DNA polymerase (Invitrogen), the cDNAs were amplified for 30 cycles (95 °C for 1 min, 58 °C for 1 min, and 72 °C for 1 min). For quantitative analysis, semi-logarithmic plots were constructed of Δ fluorescence *versus* cycle number, and a threshold was set for the changes in fluorescence at a point in the linear PCR amplification phase (C_t). The C_t values for each gene were normalized to the C_t values for β-actin with the ΔC_t equation. The level of target RNA, normalized to the endogenous reference and relative to the mock-infected and untreated cells, was calculated by the comparative C_t method with the $2^{-\Delta\Delta C_t}$ equation.

Plasmids and Transfection Assays—Reporter luciferase vectors for human full-length ICAM-1 promoter pIC1352 (−1352/+1) and the relevant mutant constructs pIC339 (−339/+1), pIC135 (−135/+1), and pIC135 (ΔAP2) have been described previously (29). To derive ICAM-1 promoter with mutated NF-κB-binding sites, the sequence of these sites was modified by two consecutive rounds of site-directed mutagenesis (QuikChange XL site-directed mutagenesis kit; Stratagene). The two NF-κB recognition sites were abrogated and changed to unique restriction sites (−187 BamHI, and −491 KpnI) in

the plasmid pIC1352 (mut2NF-κB). In the plasmid pIC339 (mutNF-κB) the -187 NF-κB-binding site was mutated and changed with BamHI restriction site. The correctness of the introduced mutations was confirmed by sequencing the derived constructs. The pGL2-ICAM-1 construct, spanning 137 nucleotides before the translation start site and carrying two Ets-responsive sites, pGL2-ICAM-1/Mut117, pGL2-ICAM-1/Mut97, and pGL2-ICAM-1/Mut117–97, the specific mutants for one or both Ets sites, respectively, have been described previously (30). The 0.4SK-pGL3 Luc, obtained by subcloning the 0.4-kb fragment of the IκBα promoter, and the relevant mutant constructs, mutkB1, mutSp1, and mutkB1/Sp1, have been described previously (31). For transfection experiments, HUVEC cells grown to subconfluence were transfected with 2 μg of the reporter vector of interest that was added to serum-free EGM-2, mixed with 6 μl of Reagent Plus and 3 μl of Lipofectamine (Invitrogen), and incubated for 2 h at 37 °C. After 4 h, the medium was replaced with EGM-2 medium containing 2% fetal bovine serum. Twenty four hours later, cells were infected with AdVIFI16 or AdVLacz (at an m.o.i. of 300) or mock-infected. After 24 h of incubation, chemiluminescence was measured using the Lumino luminometer (Stratec Biomedical Systems, Birkenfeld, Germany). Reporter gene activity was normalized to the amount of plasmid DNA introduced into the recipient cells measured by real time PCR with appropriate luciferase-actin primers.

Nuclear Extract Isolation and Electrophoretic Mobility Shift Assay (EMSA)—HUVEC were plated at a density of 3×10^5 cells/100-mm diameter dish and after 72 h infected with AdVIFI16, AdVLacz, or mock-infected. At the indicated times post-infection (p.i.), cells were washed in cold PBS, harvested, and centrifuged to collect the pellet. The pellets were then incubated for 15 min on ice with a cytoplasmic isolation buffer (10 mM HEPES (pH 7.6), 60 mM KCl, 1 mM EDTA, 1 mM dithiothreitol, 1 mM phenylmethylsulfonyl fluoride, 0.5% Nonidet P-40, protease and phosphatase inhibitor mixture (Sigma)). The samples were centrifuged, and the nuclear pellets were then collected by removing the supernatant containing the cytoplasmic extract, washed in cytoplasmic isolation buffer without Nonidet P-40, centrifuged, and incubated for 10 min on ice with a nuclear isolation buffer (20 mM Tris-HCl (pH 8.0), 420 mM NaCl, 1.5 mM MgCl$_2$, 0.2 mM EDTA, 0.5 mM phenylmethylsulfonyl fluoride, 25% glycerol, protease inhibitor mixture (Sigma)). After centrifugation, supernatants containing the nuclear extracts were collected and stored at -70 °C. EMSA was performed as described previously (32). Briefly, nuclear extracts (15 μg of proteins) were incubated in a binding buffer (10 mM Tris-HCl (pH 7.9), 50 mM NaCl, 0.5 mM EDTA, 1 mM dithiothreitol, 7.5 mM MgCl$_2$) with 1 μg of poly(dI-dC) (GE Healthcare) and the ^{32}P-labeled double-stranded NF-κB, AP-1, and Sp1 consensus oligonucleotides (Promega). The oligonucleotide probe was labeled with [γ-^{32}P]ATP (Amersham Biosciences) and T4 polynucleotide kinase according to the manufacturer's protocol, and finally column-purified on G-25 Sephadex (Bio-Rad). Complexes were analyzed by nondenaturing 4% PAGE, dried, and detected by autoradiography.

Immunoblotting—Whole-cell protein extracts were prepared by resuspending pelleted cells in lysis buffer containing 125 mM Tris-Cl (pH 6.8), 1% SDS, 20 mM dithiothreitol, 1 mM phenylmethylsulfonyl fluoride, 4 μg/ml leupeptin, 4 μg/ml aprotinin, 1 μg/ml pepstatin. After a brief sonication, soluble proteins were collected by centrifugation at $15,000 \times g$. Supernatants were analyzed for protein concentration with a D$_c$ protein assay kit (Bio-Rad) and stored at -70 °C in 10% glycerol. Proteins were separated by SDS-PAGE and then transferred to Immobilon-P membranes (Millipore). Filters were blocked in 5% nonfat dry milk in 10 mM Tris-Cl (pH 7.5), 100 mM NaCl, 0.1% Tween 20 and immunostained with the rabbit anti-IFI16 Ab (diluted 1:2000), the rabbit anti-IκBα polyclonal antibody (Santa Cruz Biotechnology) (diluted 1:500), the rabbit anti-p50 polyclonal antibody (Santa Cruz Biotechnology) (diluted 1:300), the mouse anti-p65 mAb (Santa Cruz Biotechnology) (diluted 1:500), the mouse anti-IKK2 mAb (Pharmingen) (diluted 1:1000), or the mouse anti-actin mAb (Chemicon) (diluted 1:4000). Immunocomplexes were detected with either sheep-anti mouse Ig Ab or donkey anti-rabbit Ig Ab conjugated to horseradish peroxidase (Amersham Biosciences) and visualized by enhanced chemiluminescence (Super Signal, Pierce).

IKK Kinase Assay—HUVEC cells were plated at a density of 3×10^5 cells/100-mm diameter dish and after 72 h infected with AdVIFI16, AdVLacZ, or mock-infected. At the indicated times p.i., whole-cell lysates were prepared as described previously (32, 33). Briefly, cells were resuspended in WCE lysis buffer (20 mM Tris-HCl (pH 8.0), 500 mM NaCl, 0.25% Triton X-100, 1 mM EDTA, 1 mM EGTA, 10 mM β-glycerophosphate, 10 mM NaF, 10 mM 4-nitrophenyl phosphate, 300 μM Na$_3$VO$_4$, 1 mM benzamidine, 2 μM phenylmethylsulfonyl fluoride, 1 mM dithiothreitol, protease inhibitor mixture (Sigma)) and gently rotated at 4 °C for 45 min; the lysates were centrifuged at $15,000 \times g$ for 10 min at 4 °C and then stored at -80 °C. 2 μg of anti-IKK1 mAb (Pharmingen) was added at 4 °C for 2 h. Protein A-Sepharose (GE Healthcare) was then added, and samples were incubated at 4 °C for a further 2 h. The immunoprecipitates were washed three times in WCE buffer and twice in Kinase Reaction buffer (20 mM HEPES (pH 7.7), 2 mM MgCl$_2$, 10 mM β-glycerol phosphate, 10 mM NaF, 10 mM 4-nitrophenyl phosphate, 300 μM Na$_3$VO$_4$, 1 mM benzamidine, 2 μM phenylmethylsulfonyl fluoride, 1 mM dithiothreitol, protease inhibitor mixture (Sigma)), and endogenous IKK activity was determined using GST-IκBα-(1–54) as a substrate. Kinase activity was assayed in 50 μl of KR buffer with 10 μM ATP and 5 μCi of [γ-^{32}P]ATP (Amersham Biosciences) at 30 °C for 30 min in the presence of GST-IκBα. After incubation samples were separated by SDS-PAGE, transferred to Immobilon-P membranes (Millipore), and processed for autoradiography and immunoblotting. Signals were quantitated with a densitometer. Immunoblotting analysis with anti-IKK1 mAb was performed as immunoprecipitation recovery control.

Chromatin Immunoprecipitation Assay—Cells were incubated for 10 min at room temperature with PBS containing 1% formaldehyde. Formaldehyde cross-linking was stopped by adding glycine to a final concentration of 125 mM for 5 min at room temperature. Cells were then washed with ice-cold PBS containing protease inhibitors and 1 mM phenylmethylsulfonyl fluoride and resuspended in RIPA buffer (150 mM NaCl, 1% Nonidet P-40, 0.5% deoxycholate, 0.1% SDS, 50 mM Tris-HCl

(pH 8), 5 mM EDTA) containing protease inhibitors for 20 min on ice. Samples were sonicated to reduce the DNA length to 200–600 bp, and cellular debris was removed by centrifugation. Before ChIP, the samples were precleared with protein G-agarose/carrier DNA mixture. The supernatant was recovered and used directly for immunoprecipitation experiments by incubation with appropriate antibodies for 60 min at 20 °C and then incubated for 2 h at 4 °C with protein G-agarose/carrier mixture. After immunoprecipitation, beads were collected and sequentially washed twice with 1 ml each of the following buffers: low salt wash buffer (150 mM NaCl, 1% Nonidet P-40, 0.5% deoxycholate, 0.1% SDS, 50 mM Tris-HCl (pH 8), 5 mM EDTA), high salt wash buffer (500 mM NaCl, 1% Nonidet P-40, 0.5% deoxycholate, 0.1% SDS, 50 mM Tris-HCl (pH 8), 5 mM EDTA), LiCl wash buffer (0.5% Nonidet P-40, 0.5% deoxycholate, 250 mM LiCl, 10 mM Tris-HCl (pH 8), 1 mM EDTA), and TE buffer. DNA-protein cross-links were reversed by incubation at 65 °C with 1% SDS/TE buffer. The samples were then digested with proteinase K, and DNA was recovered by phenol/chloroform/isoamyl alcohol extraction and precipitated with 2 volumes of ethanol and then resuspended in TE/RNase A buffer and incubated for 1 h at 37 °C. The input lysates were processed as above. DNA was analyzed by quantitative real time PCR using primer for the human IκBα promoter. The primers sequence used are 5′-CTA GCA GAG GAC GAA GCC AGT-3′ and 5′-CGC CTA TAA ACG CTG GCT G-3′. The amount of the DNA precipitated by the antibody was normalized to the total input DNA that was not subjected to immunoprecipitation. We assigned the value 1 to the normalized IκBα level on AdVLacZ-infected cells immunoprecipitated with unrelated antibody.

NF-κB Immunofluorescence Studies—HUVEC were seeded onto glass coverslips pretreated with 0.1% polylysine in 24-well plates and infected with AdVIFI16 or AdVLacZ at an m.o.i. of 300 or treated with TNF-α (50 ng/ml) for 24 h. The cells were then fixed in 4% phosphate-buffered paraformaldehyde for 10 min at 4 °C, permeabilized with the addition of phosphate-buffered 0.1% Triton X-100 (w/v) for 5 min at room temperature, and then incubated in PBS containing 1% bovine serum albumin (w/v, blocking solution) for 30 min. Incubation of the cells was done with either rabbit anti-human NF-κB p65 polyclonal antibodies (sc-372, Santa Cruz Biotechnology) or IFI16 mAb (1:250 dilution in blocking solution) (Santa Cruz Biotechnology) for 1 h at room temperature. This was followed by incubation with goat anti-rabbit antibodies (1:200 dilution in blocking solution) conjugated to FITC or goat anti-mouse conjugated to Texas Red (1:200) for 45 min at room temperature. Finally, the coverslips were mounted and sealed for examination under a confocal microscope (DMIRE2, Leica Microsystem, Heidelberg, Germany).

Flow Cytometry and Antibodies—HUVEC cultured in 60-mm dishes (10^4 cell/cm^2) were infected with AdVLacZ, AdVshRNAIFI16, or AdVshRNASCR or mock-infected. Sixty h.p.i cells were treated with IFN-γ (2000 units/ml) and 36 h later were collected for ICAM-1 cell surface staining. Cells were preincubated with human serum for 15 min at 4 °C to block unspecific binding, washed twice with 0.1% NaN$_3$, 0.2% bovine serum albumin in PBS, and incubated for 30 min at 4 °C with anti ICAM-1 mAb (Chemicon) followed by FITC-labeled goat anti-
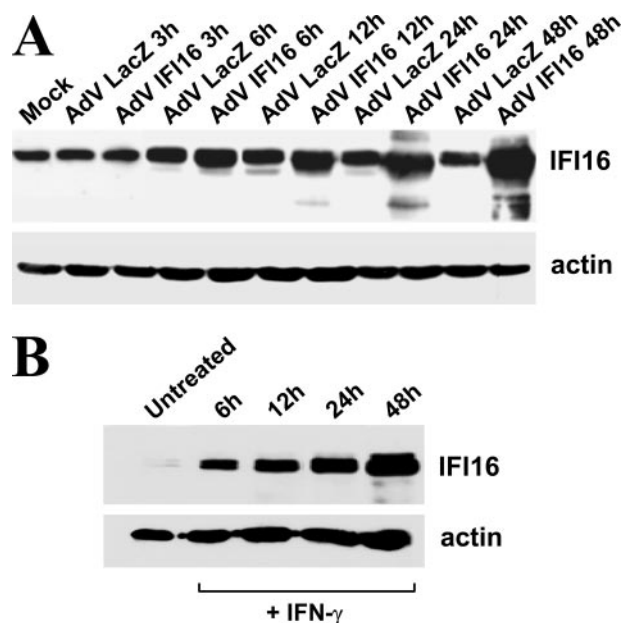

FIGURE 1. **Effects of adenovirus infection or IFN-γ treatment on IFI16 expression.** *A*, kinetics of adenovirus-mediated IFI16 overexpression. HUVECs were infected with AdVIFI16, AdVLacz (m.o.i. of 300 PFU/cell), or mock-infected. At the indicated times post-infection, total cell extracts were prepared and subjected to immunoblotting analysis with anti-IFI16 polyclonal Ab. Actin immunodetected with a mAb served as internal control. *B*, induction of IFI16 mediated by IFN-γ. HUVECs were stimulated with IFN-γ (2000 IU/ml). At the indicated times after IFN-γ treatment total cell extracts were prepared and subjected to immunoblotting analysis with anti-IFI16 Ab. Actin served as an internal control for sample loading.

mouse IgG. Negative controls consisted of isotype-matched control mAb. Labeled cells were analyzed using FACScan flow cytometer (BD Biosciences). Each analysis represented the results from at least 10^4 events.

RESULTS

IFI16 Overexpression Modifies the Gene Expression Profiles of Endothelial Cells—To investigate the effects of IFI16 overexpression on the expression of a panel of endothelial cell genes, HUVEC cells were infected with AdVIFI16 or AdVLacZ at an m.o.i. of 300 as described previously (11). As shown in Fig. 1*A*, IFI16 protein expression started to moderately increase at 6 h.p.i., continued to increase at 12 h.p.i., and peaked at 24 h.p.i. A similar pattern of IFI16 expression was observed when protein extracts from IFN-γ-treated HUVEC (2000 IU/ml) were analyzed (Fig. 1*B*). According to the kinetics results of IFI16 expression cellular mRNA was harvested at both 6 and 24 h.p.i., and RNA samples were analyzed using Sentrix human sampler arrays. This probe set is designed to detect 516 unique human transcripts divided into 7 housekeeping genes, 55 genes involved in apoptosis regulation, 38 in drugs metabolism, 82 G protein-coupled receptors, 312 in cell cycle regulation and oncogenesis, and 137 in immune system regulation. The signals were normalized to those obtained from cells expressing the control LacZ protein. Overall, the expression of 55 cellular mRNA (10.6% of the total number of mRNAs examined) was altered by IFI16 overexpression. As shown in Table 1, these genes can be grouped in five clusters as follows: 1) those genes exemplified by *MDM2* and *KPNA1* that were found increased

TABLE 1

IFI16-mediated gene expression changes in endothelial cells

GPCR indicates G protein-coupled receptors.

Gene category	Gene symbol	Description	Fold induction 6 h	Fold induction 24 h
Cancer	TYR	*Homo sapiens* tyrosinase	1.23	−0.105
	KPNA1	*H. sapiens* karyopherin α1	1.49	0.105
	CDC25A	*H. sapiens* cell division cycle 25A	2.66	0.11
	MGST1	*H. sapiens* microsomal glutathione *S*-transferase 1	0.93	0.14
	PIM1	*H. sapiens* pim-1 oncogene	0.905	0.285
	CGA	*H. sapiens* glycoprotein hormones	1.45	0.385
	LDLR	*H. sapiens* low density lipoprotein receptor	1.35	0.5
	MTHFD2	*H. sapiens* methylene tetrahydrofolate dehydrogenase	1.95	0.59
	ENG	*H. sapiens* endoglin	−1.03	−0.25
	GPX1	*H. sapiens* glutathione peroxidase 1	−0.63	0.395
	SOD1	*H. sapiens* superoxide dismutase 1	−0.06	0.57
	SSTR1	*H. sapiens* somatostatin receptor 1	0.45	3.17
	SFTPD	*H. sapiens* surfactant, pulmonary-associated protein D	0.75	2.845
	HSD3B1	*H. sapiens* hydroxy-δ-5-steroid dehydrogenase, 3β- and steroid δ-isomerase 1	0.74	2.115
	HMOX1	*H. sapiens* heme oxygenase (decycling) 1	−0.085	−0.76
	IL2RB	*H. sapiens* interleukin 2 receptor	0.215	−3.39
	UCP3	*H. sapiens* uncoupling protein 3	0.225	−2.33
	FSHR	*H. sapiens* follicle-stimulating hormone receptor	1.19	1.45
	CYP1A1	*H. sapiens* cytochrome P450	1.275	1.86
	IL1RN	*H. sapiens* interleukin 1 receptor antagonist	1.485	1.825
	EDN1	*H. sapiens* endothelin 1	−1.825	−0.865
	MKRN2	*H. sapiens* makorin, ring finger protein, 2	1.135	−0.62
	CDKN1B	*H. sapiens* cyclin-dependent kinase inhibitor 1B (p27, Kip1)	1.485	−0.975
	XRCC1	*H. sapiens* x-ray repair complementing defective repair in Chinese hamster cells 1	1.17	−1.035
	MPO	*H. sapiens* myeloperoxidase	1.92	−1.27
	LPL	*H. sapiens* lipoprotein lipase	1.355	−1.58
Immuno	STAT2	*H. sapiens* signal transducer and activator of transcription 2	1.57	0.04
	MAP2K1	*H. sapiens* mitogen-activated protein kinase kinase 1	1.015	0.13
	ICAM1	*H. sapiens* intercellular adhesion molecule 1	0.935	2.315
	CD81	*H. sapiens* CD81 antigen	−1.595	0.105
	PCP4	*H. sapiens* Purkinje cell protein 4	0.36	−1.925
	FAF1	*H. sapiens* Fas (TNFRSF6)-associated factor 1	1.36	−0.835
	CD28	*H. sapiens* CD28 antigen (Tp44)	1.695	−1.735
	CSF3R	*H. sapiens* colony-stimulating factor 3 receptor (granulocyte)	1.075	−0.535
	GADD45A	*H. sapiens* growth arrest and DNA damage-inducible, α	1.17	−0.295
	PCNA	*H. sapiens* proliferating cell nuclear antigen	1.28	0.085
	MIF	*H. sapiens* macrophage migration inhibitory factor	0.26	1.05
	CDKN2A	*H. sapiens* cyclin-dependent kinase inhibitor 2A	0.64	1.31
	JAK3	*H. sapiens* Janus kinase 3 (a protein-tyrosine kinase, leukocyte)	−0.665	−0.635
	IL7R	*H. sapiens* interleukin 7 receptor	1.85	−1.515
	CCR4	*H. sapiens* chemokine (C-C motif) receptor 4	1.42	1.61
Apoptosis	RPA3	*H. sapiens* replication protein A3, 14 kDa	1.135	0.05
	TNFSF4	*H. sapiens* tumor necrosis factor (ligand) superfamily	−0.145	−0.815
	MDM2	*H. sapiens* Mdm2	4.6	0
	BAD	*H. sapiens* BCL2-antagonist of cell death	1.15	1.35
GPCR	HRH4	*H. sapiens* histamine receptor H4	0.65	−0.325
	MC5R	*H. sapiens* melanocortin 5 receptor	1.405	−0.23
	CHRM1	*H. sapiens* cholinergic receptor, muscarinic 1	1.37	1.33
	NMU2R	*H. sapiens* neuromedin U receptor 2	1.2	0.795
	DRD2	*H. sapiens* dopamine receptor D2	1.375	−0.58
Drug metabolism	UCHL5	*H. sapiens* ubiquitin C-terminal hydrolase L5	0.955	−0.05
	NAT1	*H. sapiens* N-acetyltransferase 1 (arylamine N-acetyltransferase)	0.325	−1.825
	PON1	*H. sapiens* paraoxonase 1	1.505	−0.86
Miscellaneous	UBC	*H. sapiens* ubiquitin C	−1.605	−0.275
	EEF1A1	*H. sapiens* eukaryotic translation elongation factor 1 α1	−1.72	−0.03

at 6 h.p.i. and then returned to the basal level within 24 h; 2) those genes like *IL7R* and *CD28* that were increased at 6 h.p.i. but were decreased at 24 h.p.i.; 3) those genes like *ENG* and *EDN1* whose expression is decreased at 6 h.p.i. and then returned to the basal level at 24 h.p.i.; 4) those genes like *ICAM-1* and *CCR4* that started to increase at 6 h.p.i. and remained at an elevated level at 24 h.p.i.; and finally, 5) genes like *IL2RB* that were unaffected at 6 h.p.i. but decreased at 24 h.p.i. Some of the genes identified such as *MDM2* (*HDM2*) were previously reported to be up-regulated by *IFI16* (34), thus confirming the validity of our gene array analysis. Interestingly, as shown in Table 1, some IFI16 up-regulated genes belong to the panel of genes involved in immune system regulation and apoptosis regulation. In fact, *ICAM-1, MIF*, and *CCR4* have been implicated in the inflammatory response of endothelial

cells to microbial infections, oxidative stress, vascular disorders and tumors. Real time RT-PCR analysis (Fig. 2*A*) confirmed the gene array data indicating that *IFI16* overexpression modulates the expression of endothelial genes implicated in inflammation, cell growth, and apoptosis.

Among the genes identified by gene array analysis, we found that *IFI16* overexpression resulted in increased ICAM-1 up-regulation. Because we have previously observed that *IFI16* expression is stimulated when endothelial cells are exposed to oxidative stress or proinflammatory cytokines (11, 12), this finding prompted us to analyze if other proinflammatory molecules are induced as well. To address this hypothesis, HUVEC were infected with AdVIFI16 or AdVLacZ (m.o.i. of 300) and 18 h.p.i. mRNA were purified and analyzed by real time RT-PCR with appropriate primers. As shown in Fig. 2*B*, levels of
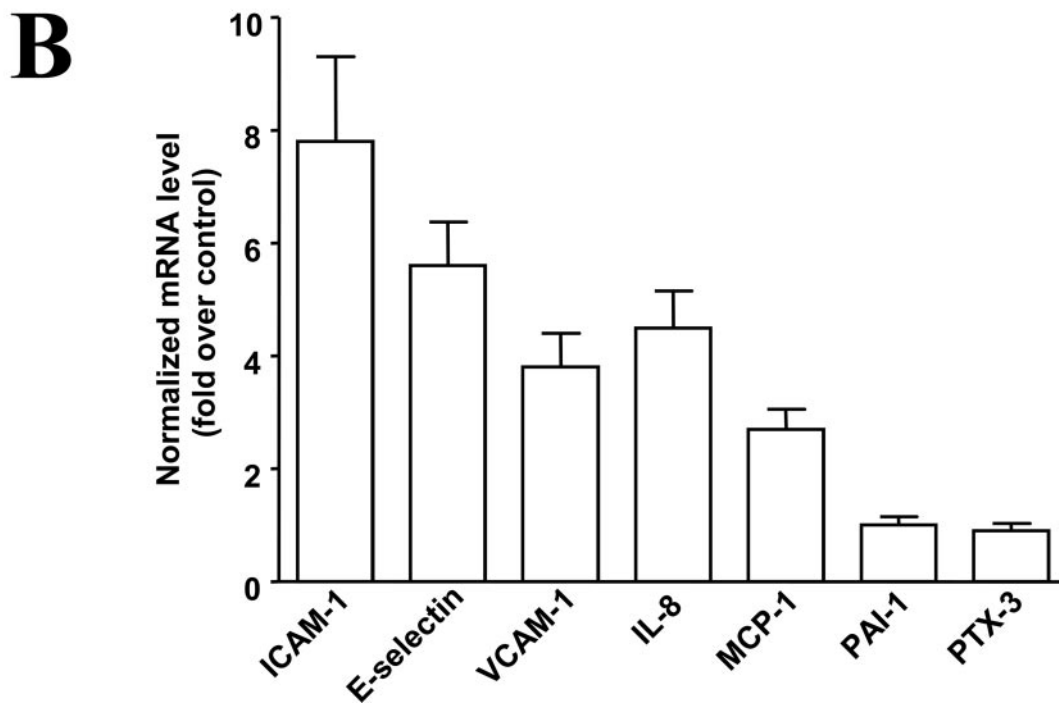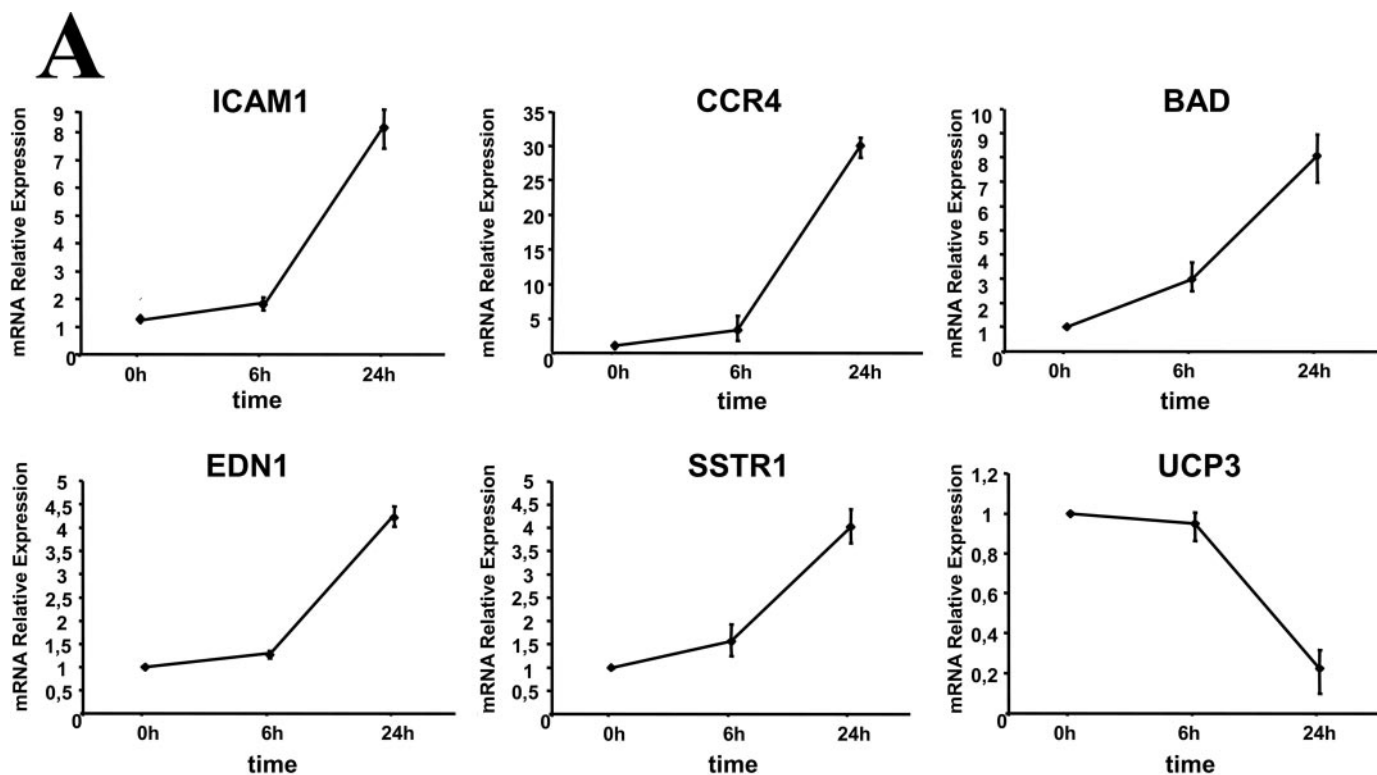
FIGURE 2. **Real time PCR analysis of AdVIFI16-infected HUVEC.** *A,* total cellular RNA was extracted from HUVEC infected with AdVIFI16 or AdVLacZ at an m.o.i. of 300 for 6 and 24 h and reverse-transcribed into cDNA, and the expression levels of indicated genes were assessed by real time PCR. The ratio of AdVIFI16/AdVLacZ infected and standardized to glyceraldehyde-3-phosphate dehydrogenase as an internal control is shown. The data shown are the values ($\pm$S.E.) from three independent experiments. *B,* total cellular RNA was extracted from HUVEC infected with AdVIFI16 or AdVLacZ at an m.o.i. of 300 for 24 h and reverse-transcribed into cDNA, and the expression levels of indicated genes were assessed by real time PCR. The ratio of AdVIFI16/AdVLacZ infected and standardized to glyceraldehyde-3-phosphate dehydrogenase (*GAPDH*) as an internal control is shown. The data shown are the values ($\pm$S.E.) from three independent experiments.

mRNA corresponding to ICAM-1, E-selectin, VCAM, IL8, and MCP-1 from AdVIFI16-infected cells were increased 7.8-, 5.5-, 3.8-, 4.3-, and 2.5-fold, respectively, compared with the same mRNA from AdVLacZ-infected HUVEC. By contrast, no induction of mRNA corresponding to PAI-1 and PTX-3 was observed, suggesting selectivity in the IFI16 activity.
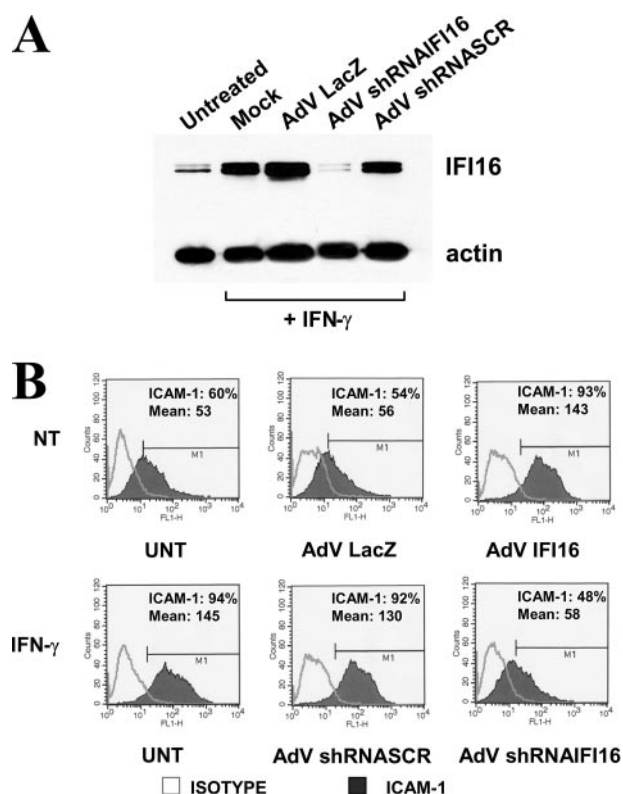
A

B

FIGURE 3. **IFI16 silencing inhibits ICAM-1 induction by IFN-γ.** HUVEC, untreated (*UNT*) or infected with the indicated adenoviral vectors for 60 h, were treated with IFN-γ (2000 units/ml) or not treated (*NT*) for 36 h and analyzed for IFI16 expression by immunoblotting (*A*) or ICAM-1 expression by FACS (*B*). Percentage of positive cells and mean of fluorescence intensity are reported in each panel. An isotype-matched antibody was used as a control. Data shown are representative of three independent experiments.

IFI16 Is Necessary and Sufficient for ICAM-1 Induction by IFN-γ—The above results suggest a role of IFI16 in the up-regulation of proinflammatory genes in endothelial cells. To evaluate the role of IFI16 in the stimulation of ICAM-1 expression in a more physiological setting, we next investigated the functional relevance of endogenous IFI16 in the IFN-γ-mediated ICAM-1 up-regulation (35, 36). To this end, endogenous IFI16 expression was inhibited before IFN-γ treatment by transduction of HUVEC cells with an AdVshRNAIFI16 that produces a specific shRNA targeted to IFI16. As shown in Fig. 3*A*, the shRNA treatment could effectively block IFI16 induction by IFN-γ at 96 h.p.i. We then measured ICAM-1 induction in the presence of IFN-γ. Upon treatment with 2000 IU/ml IFN-γ the percentage of positive cells increased from 60 to 94% with a mean fluorescence intensity ranging from 53 to 145, respectively (Fig. 3*B*). Consistent with the results of real time RT-PCR, IFI16 overexpression triggered an increase of ICAM-1-positive cells from 56% (AdVLacZ) to 93% (AdVIFI16) with a mean fluorescence intensity ranging from 56 to 143, respectively. Next, we analyzed the efficacy and specificity of shRNA to negatively interfere with IFN-γ-induced ICAM-1 expression in HUVEC. For that, prior to IFN-γ stimulation, we infected HUVEC either with IFI16 shRNA or with a scrambled shRNA serving as sequence-unrelated control. Infection with AdVshRNASCR hardly affected the extent of ICAM-1 expression upon IFN-γ treatment (92% compared with 94% with a mean fluorescence

density of 130 compared with 145). By contrast, infection with IFI16 shRNA (AdVshRNAIFI16) significantly decreased the percentage of stimulated ICAM-1 positive cells to 48% compared with HUVEC infected with AdVshRNASCR and treated with IFN-γ. The decrease in ICAM-1 positive cells was paralleled by a reduction of the mean fluorescence density from 130 (AdVshRNASCR) to 58 (AdVshRNAIFI16) (Fig. 3*B*). Taken together, these results demonstrate that in cells exposed to IFN-γ, endogenous IFI16 is the main mediator of ICAM-1 stimulation. Thus, these results underscore the potential physiological role of IFI16 in the regulation of proinflammatory genes in endothelial cells.

Identification of IFI16-responsive Elements on ICAM-1 Promoter—Next, to identify the responsive elements to IFI16, a functional analysis of the *ICAM-1* gene promoter was performed. Indicator plasmids containing ICAM-1 promoter segments progressively deleted from the 5′ end were employed. Transient transfection assays were performed with pIC1352 (−1352/+1); pIC339 (−339/+1), which contains the proximal NF-κB-binding site and the GAS site of the ICAM-1 promoter; pIC135 (−135/+1), which contains the GAS site but not the proximal NF-κB site; and pIC135 (ΔAP2), generated by the juxtaposition of a DNA segment spanning positions −135 to −105 with a fragment spanning positions −38 to +1, and thus containing the two Ets sites plus the TATA box (29, 30). As shown in Fig. 4*A*, the stimulation observed in AdVIFI16 HUVEC decreased when the DNA segment containing the 5′-flanking region of the *ICAM-1* gene was progressively shortened as in pIC339 (5-fold stimulation), pIC135 (2.5-fold), and pIC135 (ΔAP2) (2-fold). These results indicate that most of the *ICAM-1* gene promoter responsiveness (about 75%) to IFI16 expression was associated with nucleotide sequences upstream from −135 nucleotides. There have been some reports that ICAM-1 induction by IFN-γ requires NF-κB activation (35, 36) thus suggesting a possible role of NF-κB-binding sites in transcriptional regulation of *ICAM-1* promoter by IFI16. To study further the involvement of NF-κB pathway in IFI16-induced *ICAM-1* expression, transient transfection assays were performed using the human *ICAM-1* promoter-luciferase constructs, pIC1352mut2NF-κB, which contains full-length human *ICAM-1* promoter bearing two mutated κB sites or the pIC339mutNF-κB, which contains only one mutated κB site at the position −187. As shown in Fig. 4*A*, mutation of both κB sites in the full-length *ICAM-1* promoter or mutation of the single κB site in the pIC339 construct strongly decreases the capability of IFI16 to trigger luciferase activity. These results indicate that most of the *ICAM-1* promoter responsiveness (about 75%) to IFI16 is associated to κB sites demonstrating a major role of NF-κB as mediator of IFI16 activity.

The residual responsiveness of the minimal pIC135 (ΔAP2) construct to IFI16 overexpression (about 2.5-fold) (Fig. 4*A*) suggested that the Ets transcription factors may also be involved in the promoter activity regulation by IFI16. To test this hypothesis, transient transfection assays were performed with pGL2-ICAM-1, a construct that contains a region of the *ICAM-1* promoter spanning 137 nucleotides upstream from the transcriptional start site and therefore carrying the two Ets sites, or the constructs pGL2-ICAM-1mut117, pGL2-ICAM-
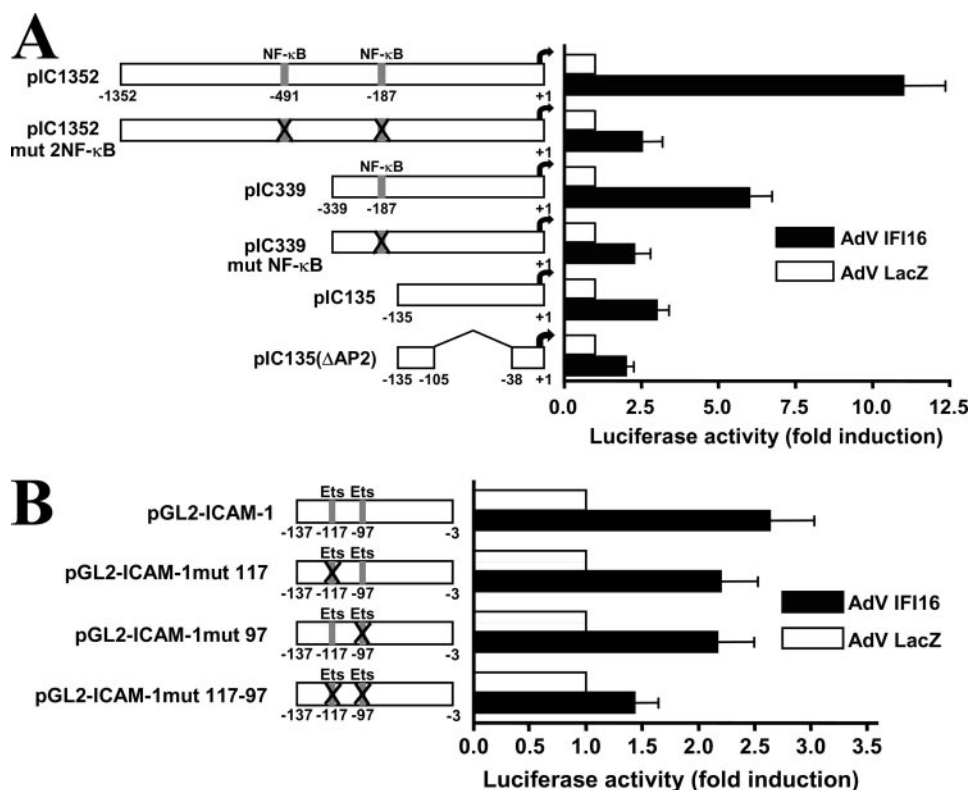
FIGURE 4. **Deletion or mutational analysis of putative IFI16-responsive elements in the *ICAM-1* promoter.** *A,* activation of pIC1352Luc and deletion mutants by IFI16. HUVEC were transfected with the indicated constructs and 24 h later infected with AdVIFI16 or AdVLacZ at an m.o.i. of 300. After an additional 36 h, protein extracts were prepared and assessed for luciferase activity. Values (±S.E.) from three independent experiments are shown, with data expressed as fold induction of promoter activity as compared with the AdVLacZ-infected cells. *B,* mutational analysis of putative Ets-responsive elements to IFI16 in the *ICAM-1* promoter. HUVEC were transfected with the indicated constructs and 24 h later infected with AdVIFI16 or AdVLacZ at an m.o.i. of 300. After an additional 36 h, protein extracts were prepared and assessed for luciferase activity. Values (±S.E.) from three independent experiments are shown, with data expressed as fold induction of promoter activity as compared with the AdVLacZ-infected cells.

1mut 97, and pGL2-ICAM-1mut 117–97, in which one or both the Ets sites were destroyed, respectively (30). As shown in Fig. 4*B*, inactivation of both Ets sites led to a further reduction of IFI16-mediated stimulation from 2.5-fold of the pGL2-ICAM-1 to 1.4-fold of pGL2-ICAM-1 mut-(117–97), thus suggesting that Ets factors contribute, albeit weakly, to the IFI16-mediated regulation of the *ICAM-1* promoter. Taken together, our results indicate that IFI16 transcriptionally activates endothelial genes involved in the inflammatory response and that this regulation is mediated primarily through activation of the NF-κB complex.

IFI16 Triggers NF-κB DNA Binding Activity—The results derived from functional analysis of the *ICAM-1* promoter prompted us to evaluate if IFI16 activates NF-κB. HUVEC were infected with AdVIFI16 or AdVLacZ, and nuclear extracts prepared for EMSA analysis using NF-κB or AP-1 consensus oligonucleotides. As shown in Fig. 5*A*, nuclear extracts from mock- or AdVLacZ-infected HUVEC cells contained low levels of NF-κB activity (*upper panel*). In contrast, a protein-DNA complex was observed in HUVEC nuclear extracts infected for 24–48 h with AdVIFI16. When the same nuclear extracts were incubated with a radiolabeled AP-1 consensus oligonucleotide, an AP-1 DNA-binding complex was observed in mock-infected cells, but the levels of this complex were not affected by either

AdVLacZ or AdVIFI16 infection, suggesting that IFI16 does not influence AP-1 DNA binding activity (Fig. 5*A*, *lower panel*).

Previous studies from our laboratory demonstrated that IFI16 interacts with p53 directly at the DNA level and increases its binding capability (11). Addition of anti-IFI16 antibodies inhibited specific p53 DNA binding as shown by supershift experiments. To assess if IFI16 interacts with NF-κB directly at the DNA level, antibodies specific for NF-κB subunits or IFI16 were added to EMSA reactions in supershift analysis. As shown in Fig. 5*B*, addition of anti-p50 and anti-p-65 antibodies supershifted the protein-DNA complex from AdVIFI16-infected cells, indicating that NF-κB p50 and p65 proteins are components of the IFI16-induced NF-κB-binding complex. In contrast, anti-IFI16 antibodies did not alter the mobility of the NF-κB complex indicating that IFI16 was not part of the protein complex interacting with the NF-κB oligonucleotide. Furthermore, coimmunoprecipitation analysis with AdVIFI16-infected HUVEC extracts confirmed the absence of a direct interaction between IFI16 and NF-κB p65 or p50 proteins (data not shown). Taken together, these results indicate NF-κB as a pivotal transducer of the IFI16 activity in terms of induction of proinflammatory molecule gene expression.

To elucidate the functional relevance of IFI16 for NF-κB binding activity induced by IFN-γ, we next examined whether ablation of IFI16 can impair NF-κB binding upon IFN-γ treatment. To this end, nuclear extracts were harvested from HUVEC infected with AdVshRNAIFI16 or AdVshRNASCR in the presence or absence of IFN-γ, and gel shift assays were performed using a NF-κB consensus oligonucleotide. As expected, NF-κB binding was induced by IFN-γ treatment compared with untreated control (*Mock*, Fig. 5*C*). By contrast, the same DNA-protein complex was significantly down-regulated when HUVEC were infected with AdVshRNAIFI16 before IFN-γ treatment. Infection with AdVshRNASCR did not impair NF-κB binding, thus demonstrating that IFI16 is the main mediator of NF-κB binding activity upon IFN-γ treatment.

IFI16 Overexpression Does Not Activate the IKK Complex but Triggers Nuclear Translocation of the NF-κB Complex—To clarify how IFI16 triggers NF-κB binding to DNA and thus its transcriptional activity, further experiments were performed to monitor the expression of NF-κB proteins and their nuclear

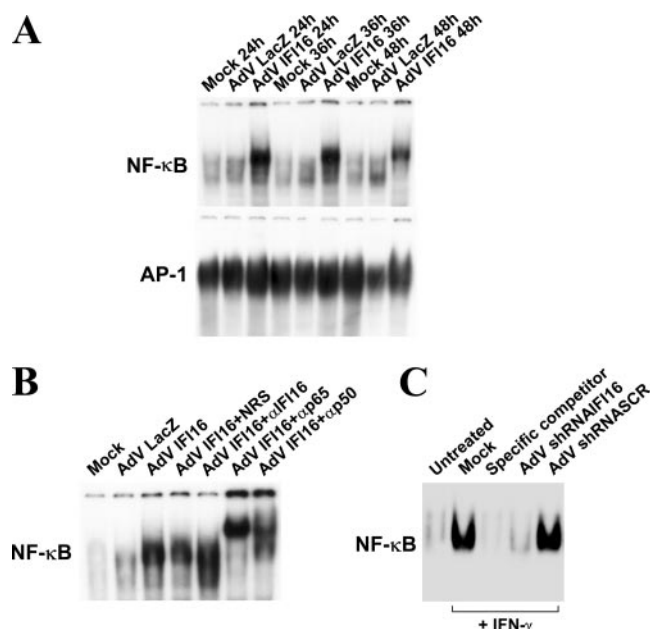# IFI16 Triggers Proinflammatory Molecule Expression

FIGURE 5. **IFI16 induces NF-κB binding.** *A,* nuclear protein extracts from HUVEC infected with AdVIFI16 or AdVLacZ at an m.o.i. of 300 for the indicated time points were incubated with radiolabeled oligonucleotides containing consensus NF-κB- (*upper panel*) or AP-1-binding sites (*lower panel*). *B,* super-shift experiments were performed by adding monoclonal antibodies against NF-κB p65 or p50 subunits, rabbit anti-IFI16 antibodies, or normal rabbit serum (*NRS*) used as a control. *C,* HUVEC, untreated or infected with the indicated adenoviral vectors for 60 h, were treated with IFN-γ (2000 units/ml) for 36 h or left untreated. Cells were then lysed, and nuclear extracts were incubated with radiolabeled oligonucleotide containing consensus NF-κB-binding sites. Competition was done with 100-fold excess of cold specific oligonucleotide. Each experiment has been repeated three times, and one representative experiment is shown.

FIGURE 6. **IFI16 does not inhibit IκBα protein expression through IKK complex phosphorylation and induces NF-κB nuclear translocation.** *A,* immunoblots of cellular lysates corresponding to AdVIFI16- or AdVLacZ-infected cells are shown. Cell lysates (20 μg/lane), prepared at the indicated time points, were separated by gel electrophoresis and transferred to Immobilon membranes. The proteins were then probed with anti-IFI16, anti-p50, anti-p65, anti-IKK2, and anti-IκBα Abs. The membrane was then incubated with the appropriate secondary Ab conjugated with horseradish peroxidase and visualized with ECL kit (Amersham Biosciences). Actin immunodetection was performed as an internal control. *B,* IFI16 does not activate the cellular IKK complex. HUVEC were left untreated, infected with AdVIFI16 or AdVLacZ at an m.o.i. of 300, or treated with TNF-α (50 ng/ml). At the indicated time points, whole-cell extracts were prepared and assayed for IKK activity using GST-IκBα as the substrate (*KA,* kinase assay) (32, 33). Endogenous IKK recovery after immunoprecipitation was determined by immunoblotting for IKK (*IB: IKK*). The experiments were repeated three times, and one representative experiment is shown.

translocation upon IFI16 overexpression. HUVEC were infected with AdVLacZ or AdVIFI16 for 24, 36, or 48 h, and immunoblotting analysis was performed on whole-cell lysates. As shown in Fig. 6*A*, IFI16 overexpression had no effect on the steady-state levels of the p50 and p65 subunits or the upstream activating IKK2 kinase, whereas it significantly decreased the levels of the inhibitory protein IκBα at all the time points examined.

The reduced levels of IκBα in cells overexpressing IFI16 prompted us to investigate whether the upstream IKK complex was activated by IFI16 thus leading to IκBα degradation. As shown in Fig. 6*B*, activation of the IKK complex (KA) was detectable only in extracts prepared from HUVEC stimulated with TNF-α (50 ng/ml for 30 min, used as a positive control), whereas no activation of the complex was detected in IFI16-overexpressing cells.

To investigate if the reduced levels of IκBα expression in the absence of the IKK complex activation were accompanied by nuclear translocation of the p50-p65 complex, we employed confocal microscopy to analyze translocation of NF-κB phosphorylated p65 subunit from the cytoplasm to the nucleus upon IFI16 overexpression. HUVEC remained either untreated (mock) or were infected with AdVLacZ or AdVIFI16 before indirect immunolabeling with anti-pan p65 antibody and FITC-coupled secondary antibodies. Pan-p65 labeling was restricted to the cytoplasm in mock and AdVLacZ-infected cells cultures (Fig. 7). By contrast, AdVIFI16-infected cells
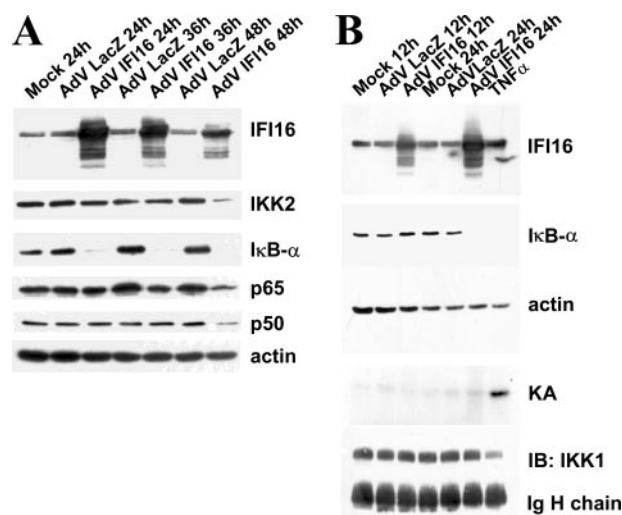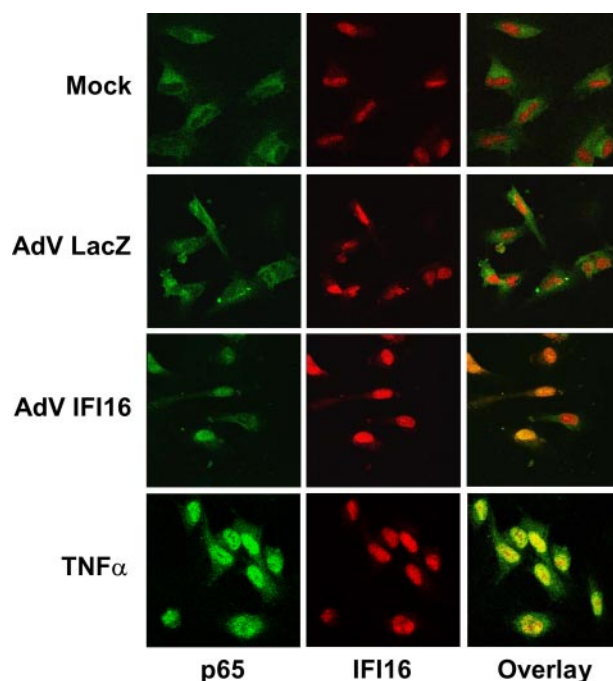

FIGURE 7. **IFI16 overexpression results in NF-κB nuclear translocation.** HUVEC, left untreated (*mock*), infected with AdVLacZ or AdVIFI16 at an m.o.i. of 300 for 24 h, or stimulated with TNF-α (50 ng/ml), were analyzed by confocal laser microscopy using an anti-pan-p65 antibody and FITC-coupled secondary antibodies, or anti-IFI16 mAb and Texas Red-coupled secondary antibodies. The experiment were repeated three times, and one representative experiment is shown.
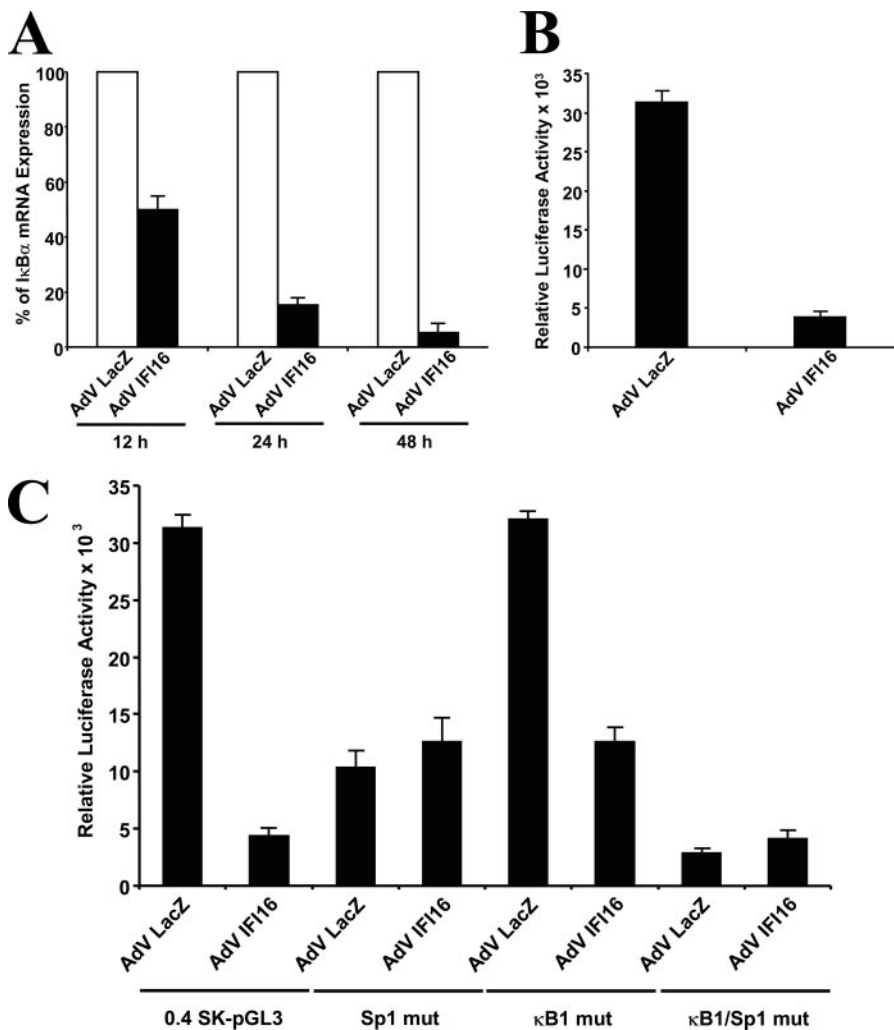
FIGURE 8. **IFI16 inhibits transcription of the *IκBα* gene.** *A*, inhibition of IκBα mRNA synthesis by IFI16. Total cellular RNA was extracted from HUVEC infected with AdVIFI16 or AdVLacZ for the indicated time periods and reverse-transcribed into cDNA, and the IκBα mRNA content was measured by real time PCR. The IκBα mRNA level standardized to glyceraldehyde-3-phosphate dehydrogenase as an internal control is as shown as percentage of AdVLacZ-infected cells. *B,* inhibition of *IκBα* gene promoter by IFI16. HUVEC were transfected with the wild-type IκBα promoter (0.4SK-pGL3Luc) and 24 h later infected with AdVIFI16 or AdVLacZ at an m.o.i. of 300. After an additional 48 h, protein extracts were assessed for luciferase activity. Values ($\pm$ S.E.) from three independent experiments are shown. *C,* Sp1 is required for suppression of IκBα promoter activity by IFI16. HUVEC were transfected with the indicated constructs, and 24 h later infected with AdVIFI16 or AdVLacZ at an m.o.i. of 300. After an additional 48 h, protein extracts were assessed for luciferase activity. Values ($\pm$ S.E.) from three independent experiments are shown.

revealed clear and intensive nuclear staining, although at a lower degree compared with the levels obtained by triggering HUVEC with TNF-α used as a positive control. Altogether, these results suggest that NF-κB activation by IFI16 is not because of the canonical NF-κB signaling pathways mediated by the IKK complex.

IFI16 Transcriptionally Suppresses IκBα Expression—In addition to activating p53-dependent transcription, full-length IFI16 fused to the heterologous GAL4 DNA binding domain can act as a potent transcriptional repressor when positioned in proximity to a promoter containing GAL4 DNA elements (37, 38). To further investigate the mechanisms that led to a reduction of IκBα steady-state levels by IFI16, we first measured by real time RT-PCR IκBα mRNA expression. As shown in Fig. 8*A*, the IκBα mRNA levels were significantly decreased (-84.7% and -94.7%, respectively) in cells infected with AdVIFI16 for

24 and 48 h compared with cells infected with the control AdVLacZ, suggesting that IFI16 overexpression reduced steady-state IκBα mRNA. To determine whether IFI16 can directly repress IκBα transcription, an indicator plasmid (p0.4K-pGL3) containing the luciferase reporter gene under the control of a region corresponding to 400 nucleotides upstream from the IκBα transcription start site was transfected into HUVEC. These cells were subsequently infected with either AdVLacZ or AdVIFI16. As shown in Fig. 8*B*, IFI16 overexpression resulted in a decrease of more than 90% luciferase activity when compared with AdVLacZ-infected HUVEC.

In vivo genomic footprinting identified the promoter-proximal NF-κB/Sp1 transcriptional switch as an essential component in the regulation of the IκBα promoter (31). To assess how IFI16 down-regulates IκBα transcription, the functional roles of the Sp1 and NF-κB sites were evaluated by transient transfection with luciferase reporter constructs driven by the wild-type IκBα promoter (0.4SK) or by mutated versions of the IκBα promoter. Point mutation of the κB1 site of the IκBα promoter (mutκB1) did not significantly impair IFI16-induced promoter suppression (Fig. 8*C*). Strikingly, point mutation of the Sp1 site (mutSp1) or mutation of both the κB1 and SP1 sites (mutκB1/SP1) relieved suppression of IκBα gene expression by IFI16.

Worthy of note, Sp1 mutation caused a significant decrease of IκBα promoter activity, consistent with its role in the basic transcription machinery (39). From these results, we conclude that a functional Sp1 site is required for suppression of IκBα promoter activity by IFI16.

Previous studies showed that IFI16 forms a stable complex with members of the Sp1/KLF family at a key DNA element located within the cytomegalovirus DNA polymerase promoter (40). To evaluate the IFI16 capability to modulate the interaction of Sp1 with the IκBα promoter nuclear extracts from AdVIFI16 or AdVLacZ-infected, cells were analyzed by EMSA. As shown in Fig. 9*A* (*lanes 1, 2, 4,* and *5*), the oligonucleotide spanning the Sp1-binding site formed a major complex with nuclear extracts from both mock cells or cells infected with AdVLacZ 12 and 24 h.p.i., respectively. This complex was specifically competed by a 100-fold higher concentration of the
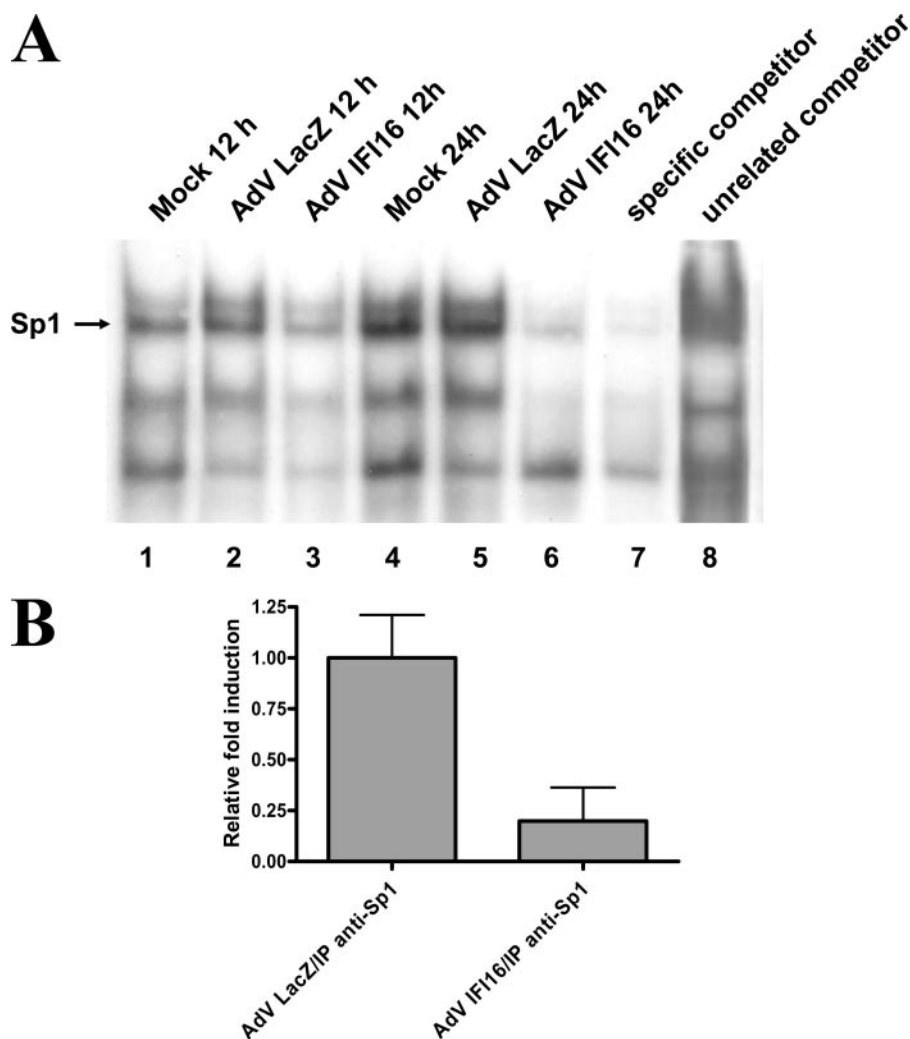
FIGURE 9. **Suppression of Sp1 binding to the IκBα promoter by IFI16.** *A,* nuclear protein extracts from HUVEC infected with AdVIFI16 or AdVLacZ at an m.o.i. of 300 for the indicated time points were incubated with a radiolabeled oligonucleotide containing a consensus Sp1-binding site. Competitions were done with 100-fold excess of cold oligonucleotides, and 1 μg of polyclonal antibodies were employed for supershift experiments. Each experiment has been repeated three times, and one representative experiment is shown. *B,* displacement of Sp1 from the IκBα promoter in AdVIFI16-infected HUVEC was analyzed by ChIP assay using anti-Sp1 rabbit polyclonal antibodies. Sp1-coprecipitating DNA was analyzed by quantitative real time PCR with promoter-specific primers amplifying the IκBα promoter. An unrelated rabbit polyclonal antiserum was used as control. Genomic DNA obtained from AdVLacZ- or AdVIFI16-infected cells was employed to normalize the DNA subjected to immunoprecipitation (input).

nocomplexes was analyzed by quantitative real time PCR to detect the enrichment of the IκBα promoter sequences in the immunoprecipitates. The rate of amplification was verified using cross-linked, not immunoprecipitated chromatin (INPUT). The specificity of chromatin immunoprecipitation was determined by using a control unrelated antibody. Consistent with EMSA results, real time PCR analysis of the purified ChIPed DNA showed indeed that Sp1 antibody pulled down significantly more Sp1-bound IκBα promoter DNA in extracts from AdVLacZ-infected HUVEC compared with those from AdVIFI16-infected HUVEC (Fig. 9*B*). Unrelated, affinity-purified polyclonal antibodies, used as negative control, did not immunoprecipitate the complex containing the IκBα promoter (not shown). Altogether, these findings indicate that the suppression of IκBα gene transcription in the presence of IFI16 is because of an inhibition of the of Sp1 recruitment to its promoter.

Negative Regulation of IκBα by Specific siRNA Results in NF-κB Activation—To examine whether direct inhibition of IκBα expression by specific siRNA resulted in the same outcome observed with IFI16, HUVEC were infected with AdVshIκBα for 48, 72, or 96 h, and IκBα mRNA was analyzed by quantitative RT-PCR. As shown in Fig. 10*A*, IκBα mRNA levels were significantly decreased at 96 h.p.i. compared with mock or AdVsh-RNASCR-infected cells. These data were also confirmed by immunoblotting analysis (Fig. 10*B*).

To verify whether this decrease of IκBα was accompanied by NF-κB activation, HUVEC, infected with AdVshRNAIκBα, AdVshRNASCR, or AdVIFI16, were analyzed for DNA binding activity by EMSA. As shown in Fig. 10*C*, a protein-DNA complex was observed in nuclear extracts from HUVEC infected for 96 h with AdVshRNAIκBα or with AdVIFI16 for 24 h. By contrast, a barely retarded complex was observed with nuclear extracts from HUVEC left untreated (mock) or infected with AdVshRNASCR. To definitively prove that the retarded complex contained NF-κB components, antibodies specific for p65 or p50 NF-κB subunits were added to EMSA reactions in supershift analysis. As shown in Fig. 9*C*, addition of anti-p50 and anti-p-65 antibodies supershifted the protein-DNA complex from AdVshRNAIκBα-infected cells, indicating that both

unlabeled oligonucleotide (Fig. 9*A, lane 7*) but not by the same concentration of a mutated oligonucleotide (*lane 8*). By contrast, when nuclear extracts from AdVIFI16-infected HUVEC were incubated with the labeled Sp1 oligonucleotide, the Sp1 binding activity was significantly reduced at both 12 and 24 h.p.i. (Fig. 9*A, lanes 3* and *6*) suggesting that IFI16 inhibits Sp1 DNA binding to the IκBα promoter. Altogether, these results demonstrate that suppression of IκBα transcription by IFI16 is accompanied by displacement of Sp1-like factors from its promoter.

To further support this hypothesis, the binding of Sp1 to the IκBα promoter in the presence of IFI16, was then analyzed *in vivo* by ChIP assay. Formaldehyde cross-linked, sonicated chromatin fragments from HUVEC infected with AdVIFI16 or AdVLacZ 24 h earlier were immunoprecipitated with an anti-Sp1 polyclonal antibody. Then the DNA released from immu-
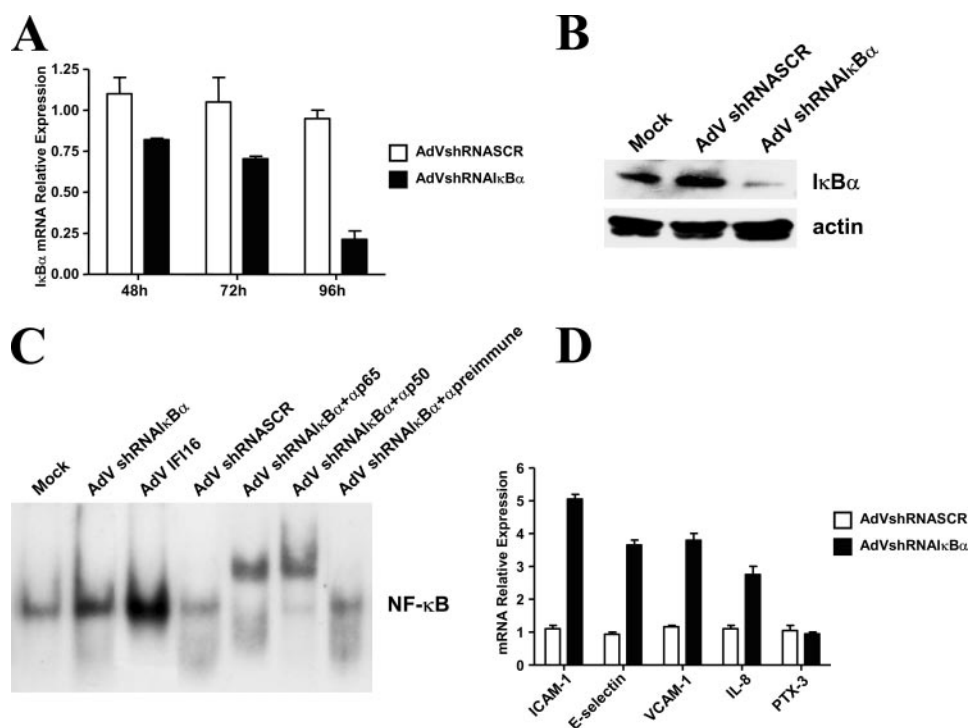
FIGURE 10. **IκBα silencing triggers NF-κB activation and gene-dependent induction.** HUVEC, left untreated (mock) or infected with AdVsiRNAIκBα, AdVsiRNASCR, or AdVIFI16, were analyzed for IκBα mRNA (*A*) and protein expression (*B*) by real time RT-PCR and immunoblotting, respectively. DNA binding activity was measured using radiolabeled oligonucleotides containing a consensus NF-κB binding region (*C*). *D*, real time RT-PCR analysis of RNA expression of the indicated genes. Data shown are representative of three independent experiments.

NF-κB p50 and p65 proteins are components of the NF-κB-binding complex induced by IκBα knockdown.

NF-κB activation by IFI16 resulted in the induction of genes, such as *ICAM-1,* E-selectin, *VCAM-1,* and *IL-8* all containing NF-κB-binding sites in their promoter region (Fig. 2) (20–22). To verify if down-regulation of IκBα followed by NF-κB nuclear translocation and binding to DNA resulted in the same outcome, HUVEC were infected with AdVshRNAIκBα or AdVshRNASCR for 96 h (m.o.i. 1000), mRNA-purified, and analyzed by real time RT-PCR with appropriate primers. As shown in Fig. 10*D*, the levels of mRNA corresponding to ICAM-1, E-selectin, VCAM-1, and IL8 from AdVshIκBα-infected HUVEC were increased of 4.8-, 3.2-, 3.5-, and 2.4-fold, respectively, compared with the same mRNA from AdVshSCR-infected cells, whereas no induction of mRNA corresponding to PTX-3 was observed. Altogether, these results demonstrate that IκBα negative regulation by specific siRNA results in an outcome similar to that observed with IF16 overexpression.

DISCUSSION

Human IFI16, the interferon-inducible p200 family protein, modulates various cellular responses as follows: inhibits cell proliferation, modulates p53-mediated apoptosis, stimulates senescence in fibroblasts and epithelial cells, plays a role in the differentiation of CD34+/CD38− stem cells, and inhibits tube morphogenesis of primary endothelial cells (4–6, 38). In this study, we identify a novel role for IFI16 as inducer of the first steps of inflammation. The major finding is that IFI16 triggers ICAM-1 expression by activating the NF-κB complex through a previously unraveled mechanism, *i.e.* transcriptional suppression of IκBα.

The analysis of gene expression using DNA microarrays can help to understand molecular pathways at the cellular level and can correlate them with cellular functions such as cell proliferation, differentiation, and apoptosis (41, 42). This analysis revealed modulation of genes involved in various functions, including cell cycle arrest, apoptosis, cell proliferation, and differentiation. To validate the gene changes, 6 different genes from the 55 genes that displayed <0.5- and >2-fold changes on macroarray analysis were selected for real time RT-PCR analysis. Among the various genes, *ICAM-1* was up-regulated following IFI16 overexpression. Together with the observation that IFI16 expression is stimulated in HUVEC by proinflammatory cytokines or oxidative stress (11, 12), this finding prompted us to investigate if other proinflammatory molecules, such as E-selectin, IL-8, and MCP-1, are induced as well. The results obtained by real time RT-PCR analysis demonstrated that IFI16 overexpression stimulates indeed their expression. As such, these studies identify IFI16 as a novel regulator of endothelial cell proinflammatory gene activation.

IFNs stimulate expression of a large group of immune modulating genes that play a role both in innate and acquired immune responses. These genes include chemokines and adhesion molecules that are involved in the recruitment of lymphocytes to the site of inflammation and adherence to infected cells (18, 43). In this context, our observation that IFI16 can stimulate ICAM-1, E-selectin, IL-8, and MCP-1 expression is of considerable interest, inasmuch as it now identifies the *IFI16* gene as one of the mediators of IFN immunomodulatory activities. In this study, FACS analysis showed an ICAM-1 expression after IFN-γ stimulation of 94% compared with 60% in unstimulated HUVECs. After transduction with IFI16-specific shRNA, the stimulated expression of ICAM-1 on the cell surface could be diminished to 48%. The minor reduction of ICAM-1 expression seen upon transduction with scrambled shRNA demonstrates the specificity of the IFI16 activity and the potency of the shRNAIFI16 to suppress the expression of the ICAM-1 adhesion molecules in endothelial cells. Taken together, these results support the hypothesis that silencing of IFI16 expression in endothelial cells may represent a promising approach for modulating the induction of proinflammatory molecules by IFNs, one of the initial steps of inflammatory processes that precede the onset of autoimmune syndromes.

The process of endothelial activation underlies tight regulatory control mechanisms (17). Proinflammatory stimuli target-

The Journal of Biological Chemistry

ing the endothelium, such as IFNs, TNF-α, IL-1β, or bacterial lipopolysaccharides, elicit activation of intracellular signal transduction cascades. An important consequence of these stimuli is the activation of members of the NF-κB complex. In fact, NF-κB was implicated as the major transcriptional regulator of endothelial adhesion molecules, including ICAM-1, E-selectin, and chemokines, including IL-8 and MCP-1. Consistent with these observations IFI16 triggers expression of proinflammatory genes by activating the NF-κB complex. Until now, three distinct NF-κB-activating pathways have emerged, and all of them rely on sequentially activated kinases (22–26, 44). Our studies show that IFI16 is an important regulator of NF-κB activity through an alternative pathway independent from cytoplasmic kinases that lead to the suppression of *IκBα* gene transcription and thus allow nuclear translocation of NF-κB proteins. This conclusion is based on the following lines of evidence. First, the levels of IκBα expression at both protein and mRNA levels decrease upon IFI16 overexpression. Second, IFI16 knockdown impairs NF-κB binding to DNA triggered by IFN-γ. Third, point mutations introduced at the Sp1-binding sites of the IκBα promoter and crucial for the basal gene activity resulted in an impaired IFI16-mediated promoter suppression. Finally, both EMSA and ChIP assays demonstrated that Sp1 binding to the IκBα promoter sequences is inhibited by IFI16 overexpression. The mechanisms responsible for the displacement of Sp1 by IFI16 to the IκBα promoter are unknown at the moment. IFI16 has been demonstrated to form a stable complex with the cellular transcriptional activators of the Sp1/KLF factor family at a key DNA element (inverted repeat 1 (IR1)) located within the cytomegalovirus DNA polymerase gene promoter (40). IFI16 was able to repress transcription of a reporter gene containing wild-type IR1 within the upstream promoter, whereas mutation of IR1, resulting in loss of binding of the Sp1-IFI16 complex, caused a loss of IFI16-mediated transcriptional repression (37). In our experimental setting, we could not demonstrate this type of protein-protein interaction,[3] but this may be due to relative labile binding between IFI16 and Sp1. An intriguing alternative mechanism may be an indirect interaction in such a way that IFI16 specifically binds to and squelches certain (co)factors, necessary for the Sp1 transcription factor(s) to enhance transcription. Our data suggest that the negative regulation imposed by IFI16 on IκBα transcription is independent of alterations in the IKK complex kinetic activity. Support for these findings comes from the observation that reduction in IκBα expression levels by specific siRNA results in the same outcome (Fig. 10, *C* and *D*). Although modulation of IκBα expression has been shown previously to be a mechanism explaining altered NF-κB activity (22–27), our study is unique as we propose a molecular mechanism behind modulated NF-κB activity by which IκBα protein stability is altered via gene transcription and is thus independent of alterations in IKK complex kinetic activity.

The existence of a positive interaction between IFI16 and NF-κB transcription factor may have far reaching implications, because many genes that play a role in host defense mecha-

nisms contain NF-κB elements in their promoter region and therefore could explain the profound, although largely unexplained, harmful effects of IFI16 on the immune system. IFI16 and the mouse homologue Ifi202a have indeed been implicated in the etiology and pathology of systemic lupus erythematosis (45, 46). High titer anti-IFI16 antibodies were detected in the sera of 28.7% systemic lupus erythematosus patients but not in healthy controls. A markedly high frequency of anti-IFI16 autoantibodies was also observed in the sera of another autoimmune disease, Sjogren syndrome (47). Consistent with these results we have observed that anti-IFI16 antibodies are present in the sera of 26.5% patients affected by systemic scleroderma (16). Interestingly, in accordance with the finding that IFI16 expression is observed in squamous epithelia of the epidermis, the anti-IFI16 antibodies correlate with the limited cutaneous form of scleroderma.

In summary, our studies assign to IFI16 a novel role in the signal transduction pathways regulating the inflammation processes and provide a more complete understanding of how induction of proinflammatory molecules may result in the onset of autoimmunity.

REFERENCES

1. Bekisz, J., Schmeisser, H., Hernandez, J., Goldman, N. D., and Zoon, K. C. (2004) *Growth Factors* **22,** 243–251
2. Parmar, S., and Platanias, L. C. (2005) *Cancer Treat. Res.* **126,** 45–68
3. Kong, J. S., Teuber, S. S., and Gershwin, M. E. (2006) *Autoimmun. Rev.* **5,** 471–485
4. Asefa, B., Klarman, K. D., Copeland, N. G., Gilbert, D. J., Jenkins, N. A., and Keller, J. R. (2004) *Blood Cells Mol. Dis.* **32,** 155–167
5. Landolfo, S., Gariglio, M., Gribaudo, G., and Lembo, D. (1998) *Biochimie (Paris)* **80,** 721–728
6. Ludlow, L. E. A., Johnstone, R. W., and Clarke, C. J. P. (2005) *Exp. Cell Res.* **308,** 1–17
7. Inohara, N., and Nunez, G. (2003) *Nat. Rev. Immunol.* **3,** 371–382
8. Tschopp, J., Martinon, F., and Burns, K. (2003) *Nat. Rev. Mol. Cell Biol.* **4,** 95–104
9. Aglipay, J. A., Lee, S. W., Okada, S., Fujiuchi, N., Ohtsuka, T., Kwak, J. C., Wang, Y., Johnstone, R. W., Deng, C., Qin, J., and Ouchi, T. (2003) *Oncogene* **22,** 8931–8938
10. Albrecht, M., Choubey, D., and Lengauer, T. (2005) *Biochem. Biophys. Res. Commun.* **327,** 679–687
11. Gugliesi, F., Mondini, M., Ravera, R., Robotti, A., De Andrea, M., Gribaudo, G., Gariglio, M., and Landolfo, S. (2005) *J. Leukocyte Biol.* **77,** 820–829
12. Mondini, M., Vidali, M., Airò, P., De Andrea, M., Riboldi, P. S., Meroni, P. L., Gariglio, M., and Landolfo, S. (2007) *Ann. N. Y. Acad. Sci.* **1110,** 47–56
13. Gariglio, M., Azzimonti, B., Pagano, M., Palestro, G., De Andrea, M., Valente, G., Voglino, G., Navino, L., and Landolfo, S. (2002) *J. Interferon Cytokine Res.* **22,** 815–821
14. Wei, W., Clarke, C. J., Somers, G. R., Gresswell, K. S., Loveland, K. A., Trapani, J. A., and Johnstone, R. W. (2003) *Histochem. Cell Biol.* **119,** 45–54
15. Raffaella, R., Gioia, D., De Andrea, M., Cappello, P., Giovarelli, M., Marconi, P., Manservigi, R., Gariglio, M., and Landolfo, S. (2004) *Exp. Cell Res.* **293,** 331–345
16. Mondini, M., Vidali, M., De Andrea, M., Azzimanti, B., Airò, P., Riboldi, P. S., Meroni, P. L., Albano, E., Shoenfeld, Y., Gariglio, M., and Landolfo, S. (2006) *Arthritis Rheum.* **54,** 3939–3944

---

[3] S. Landolfo, unpublished results.

17. Cook-Mills, J. M., and Deem, T. L. (2005) *J. Leukocyte Biol.* **77,** 487–495
18. Millan, J., Hewlett, L., Glyn, M., Toome, D., Clark, P., and Ridley, A. J. (2006) *Nat. Cell Biol.* **8,** 113–123
19. Muller, W. A. (2003) *Trends Immunol.* **24,** 327–334
20. Denk, A., Goebeler, M., Schmid, S., Berberich, I., Ritz, O., Lindemann, D., Ludwig, S., and Wirth, T. (2001) *J. Biol. Chem.* **276,** 28451–28458
21. Kempe, S., Kestler, H., Lasar, A., and Wirth, T. (2005) *Nucleic Acids Res.* **33,** 5308–5319
22. Bonizzi, G., and Karin, M. (2004) *Trends Immunol.* **25,** 280–288
23. Li, X., and Stark, G. R. (2002) *Exp. Hematol.* **4,** 285–296
24. Karin, M., and Greten, F. R. (2005) *Nat. Rev. Immunol.* **5,** 749–759
25. Janssens, S., and Tschopp, J. (2006) *Cell Death Differ.* **13,** 1–12
26. Kato, T., Jr., Delhase, M., Hoffman, A., and Karin, M. (2003) *Mol. Cell* **12,** 829–839
27. Viatour, P., Merville, M.-P., Bours, V., and Chariot, A. (2005) *Trends Biochem. Sci.* **30,** 43–52
28. Mittereder, N., March, K. L., and Trapnell, B. C. (1996) *J. Virol.* **70,** 7498–7509
29. Van de Stolpe, A., Caldenhoven, E., Stade, B. G., Koenderman, L., Raaijmakers, J. A., Johnson, J. P., and van der Saag, P. T. (1994) *J. Biol. Chem.* **269,** 6185–6192
30. de Launoit, Y., Audette, M., Pelczar, H., Plaza, S., and Baert, J. L. (1998) *Oncogene* **16,** 2065–2073
31. Algarté, M., Kwon, H., Génin, P., and Hiscott, J. (1999) *Mol. Cell. Biol.* **19,** 6140–6153
32. Caposio, P., Dreano, M., Garotta, G., Gribaudo, G., and Landolfo, S. (2004) *J. Virol.* **78,** 3190–3195
33. Mercurio, F., Zhu, H., Murray, B. W., Shevchenko, A., Bennet, B. L., Li, J. W., Young, D. B., Barbosa, M., Mann, M., Manning, A., and Rao, A. (1997) *Science* **278,** 860–866
34. Fujiuchi, N., Aglipay, J. A., Ohtsuka, T., Maehara, N., Sahin, F., Su, G. H., Lee, S. W., and Ouchi, T. (2002) *J. Biol. Chem.* **279,** 20339–20344
35. Chang, Y. J., Holtzman, M. J., and Chen, C. C. (2004) *Mol. Pharmacol.* **65,** 589–598
36. Chang, Y. J., Holtzman, M. J., and Chen, C. C. (2002) *J. Biol. Chem.* **277,** 7118–7126
37. Johnstone, R. W., Kerry, J. A., and Trapani, J. A. (1998) *J. Biol. Chem.* **273,** 17172–17177
38. Johnstone, R. W., and Trapani, J. A. (1999) *Mol. Cell. Biol.* **19,** 5833–5838
39. Black, A. R., Black, J. D., and Azizkhan-Clifford, J. (2001) *J. Cell. Physiol.* **188,** 143–160
40. Luu, P., and Flores, O. (1997) *J. Virol.* **71,** 6683–6691
41. Schena, M., Shalon, D., Davis, R. W., and Brown, P. O. (1995) *Science* **270,** 467–470
42. Shalon, D., Smith, S. J., and Brown, P. O. (1996) *Genome Res.* **6,** 639–645
43. Kunkel, E., and Butcher, E. C. (2003) *Nat. Rev. Immunol.* **3,** 822–829
44. Tergaonkar, V., Correa, R. G., Ikawa, M., and Verma, I. M. (2005) *Nat. Cell Biol.* **7,** 921–923
45. Rozzo, S. J., Allard, J. D., Choubey, D., Vyse, T. J., Izui, S., Peltz, G., and Kotzin, B. L. (2001) *Immunity* **15,** 435–443
46. Seelig, H. P., Ehrfeld, H., and Renz, M. (1994) *Arthritis Rheum.* **37,** 1672–1683
47. Uchida, K., Akita, Y., Matsuo, K., Fujiwara, S., Nakagawa, A., Kazaoka, Y., Hachiya, H., Naganawa, Y., Oh-iwa, I., Ohura, K., Saga, S., Kawai, T., Matsumoto, Y., Shimozato, K., and Kozaki, K.-I. (2005) *Immunology* **116,** 53–63